COBEM 2023 27TH INTERNATIONAL CONGRESS OF MECHANICAL ENGINEERING

ABCM Brazilian Society of Mechanical Sciences and Engineering
27th ABCM International Congress of Mechanical Engineering
December 04-08, 2023, Florianópolis-SC, Brazil

COB-2023-2433
NUMERICAL SIMULATIONS OF THE HELICON PLASMA THRUSTER EXPERIMENT UNDER DIFFERENT MAGNETIC CONFIGURATIONS

Renan A. de Souza
Rodrigo A. Miranda
José L. Ferreira
University of Brasilia (UnB), UnB-Gama campus, Brasilia, DF 72.444-240 Brazil.
souzaalmeidarenan@gmail.com
rmiracer@gmail.com
leonardoferreira@unb.br

Abstract. *This paper reports the latest findings from the Helicon Plasma Thruster experiment being developed at the University of Brasilia (HPT-UnB). This device employs a radiofrequency (RF) antenna to generate plasma within a glass tube containing a dielectric material, linked to a wider tube with a flange. Magnetic coils maintain a constant field within the tube, including its diverging end. The interaction with this magnetic field generates internal structures that control power coupling and plasma diffusion in the magnetic nozzle section. Recently, the HPT-UnB setup was updated by introducing movable rails for the magnetic coils, allowing parametric studies by adjusting their position relative to the RF antenna and altering the coil spacing. Additionally, the metal flange connecting the tubes was replaced with a dielectric material to prevent particle loss. Updates were made to the particle-in-cell model to reflect these changes. These preliminary results are crucial for identifying key parameters and validating the experimental engine at the Laboratory of Plasma Physics, University of Brasilia (LFP-UnB).*

Keywords: *Propulsion, plasma, helicon waves, plasma thruster, plasma simulation*

1. INTRODUCTION

Recently, there has been a growing interestin a variety of electrodeless plasma sources for electric propulsion. The HPT has been considered an efficient alternative among the vast variety of thrusters such as the PPT and the MPD thrusters, which are classified as electrode thrusters and are prone to erosion, resulting in a shorter operational lifetime (Godyak, 2020). Numerical simulations and experiments have allowed a deeper understanding of the HPT behaviour and application (Miranda *et al.*, 2019) (Pottinger *et al.*, 2011) (Takahashi *et al.*, 2011) (Williams and Walker, 2013).

The operation of the HPT can be described briefly as follows. A neutral gas is pumped into a cylindrical glass tube. Helicon waves are emitted by a radiofrequency antenna, which ionizes the gas. A magnetic field aligned with the axial direction is generated along the tube by a set of coils. The magnetic field confines the plasma to the center of the tube and generates a magnetic nozzle configuration near the exit region. Therefore, the system does not require any external neutralizers or electrodes, resulting in a simpler system to be constructed (Godyak, 2020).

The HPT consists of an ion azimuthal acceleration antenna and a magnetic nozzle, which provides thrust through an insulated source tube and a magnetic field to achieve plasma confinement and produce plasma expansion, converting azimuthal and radial plasma motion into axial motion. Gases such as argon, xenon and helium can be employed to produce thrusts up to 10 mN (Charles, 2007).

The LFP-UnB is currently developing a numerical model of a prototype of an HPT to validate the experimental tests held in the past few years, according to Miranda *et al.* (2019). The prototype has been recently updated to allow for parametric studies based on the position and the distance between the magnetic coils. Figure 1 shows a simplified diagram of the experiment.

The organization of this paper follows. Section 2 describes the experimental device, the numerical model and the simulation code. Section 3 presents the numerical results, and Section 4 presents the conclusions of this work.

2. THE HPT-UNB EXPERIMENT

2.1 Experimental device and updates

Figure 1 shows a diagram of the experimental device. Two glass tubes with different diameters are connected through a dielectric flange. The electromagnetic coils and the RF antenna are located at a position in a glass tube with smaller diameter. Argon gas is injected from the right-hand side of the tube with the coils, and plasma is produced by setting the antenna to 13.56 MHz. The magnetic field from the coils confine the plasma at the centre of the tube, and most of the

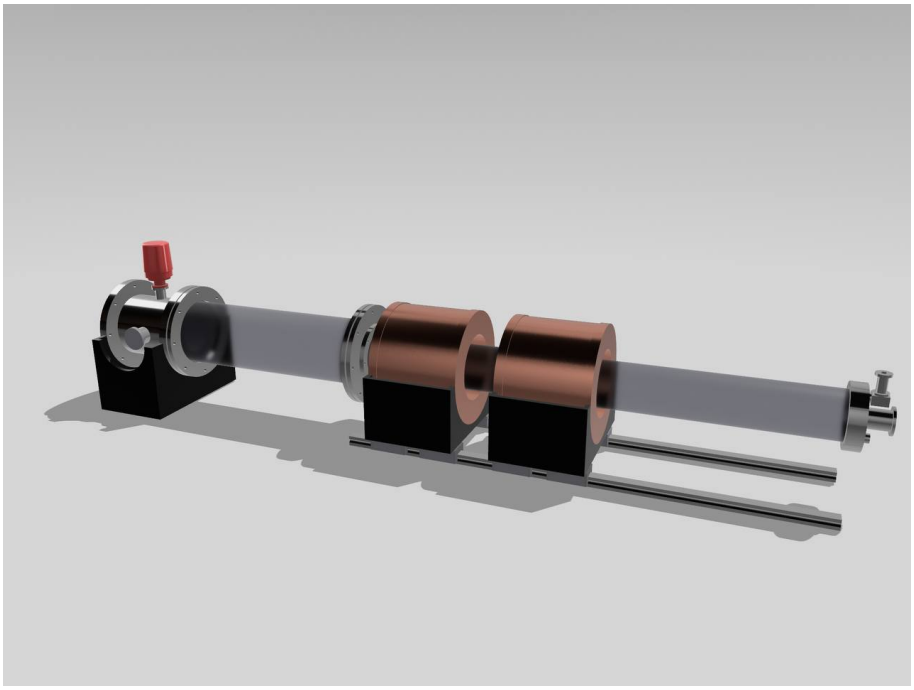

Figure 1. The design of the HPT-UnB Experiment.

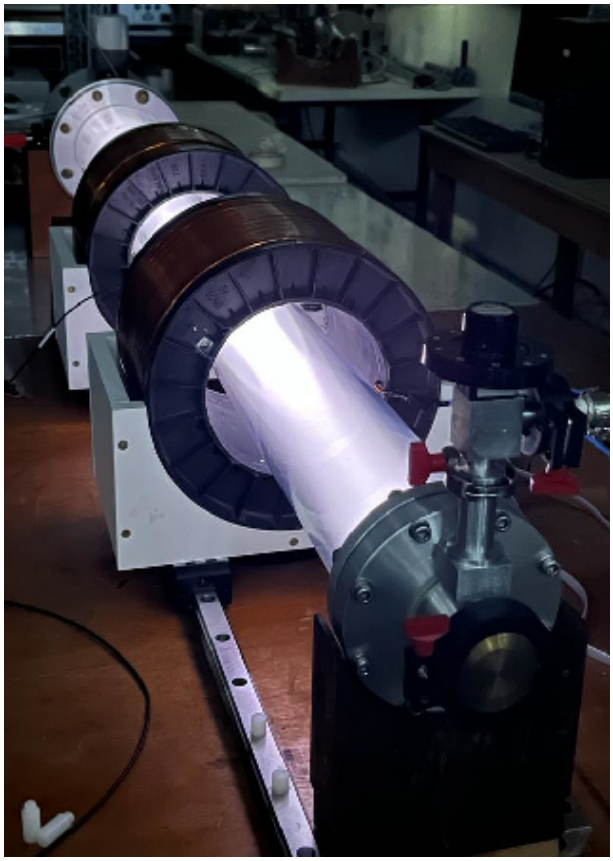

Figure 2. The experiment under operation at LFP-UnB.

particles propagate towards the wider glass tube.

The experiment has been updated from its original configuration Miranda *et al.* (2019) by installing metallic rails supporting the electromagnetic coils. The rails allow the coils to move freely in the axial direction throughout the length of the right-hand tube. The rails also allow us to fix the position of the coils at any position. Currently it has been performed parametric studies on the dynamics of the confined plasma as a function of the position of the coils. These

studies aim to find an optimal configuration of the HPT-UnB.

The electromagnetic coils have been also updated to allow us to set the current circuitry independently to each other. This allows us to set the coil currents in different directions and investigate different modes of operation such as an asymmetric mode, in which the current of each coil is set to different values, and the cusp-mode, in which the coil currents are set to opposite directions, and the resulting magnetic field is of opposing polarity.

A photograph of the experimental device under operation is shown in Fig. 2. This test was conducted using a wave generator operating at 17 MHz. During this test the rails were demonstrated to work properly and the plasma displayed different dynamical behaviour depending on the position of the coils throughout the glass tube.

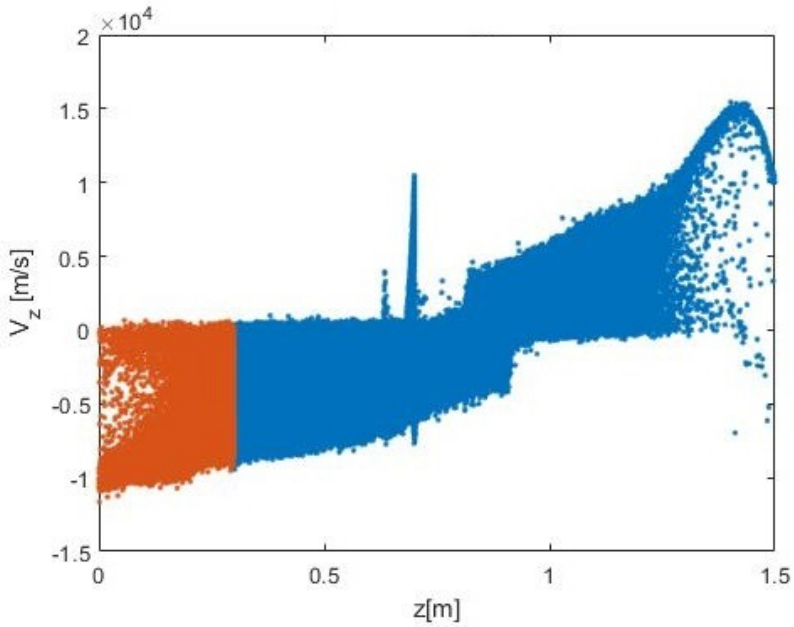

Figure 3. The axial component v_z of the ion velocity as a function of z, for the second configuration of Table 1. Particles in the orange colour are near the exit region.

The metallic flanges have been replaced for a new material, polyacetal, to avoid a loss of particles to the flange observed in Miranda *et al.* (2019). For example, in Fig. 3, at z = 0.7 a number of ions are attracted to the metallic flange.

2.2 Particle-in-cell model

A two-dimensional model of the HPT-UnB is defined by using cylindrical coordinates and keeping the (z, r) coordinates (i.e., neglecting variations along the azimuthal direction). The simulation domain shown in Fig. 3 takes into account the upper half of a cross-section of the HPT, due to its symmetry. The walls of the glass tubes are represented by regions with a dielectric permittivity of 4.7.

The metal chamber at the end of the device is represented with a conducting boundary. Figure 4 also displays the location of the pair of coils, consisting of 710 loops of copper wire with a 3 mm diameter. The magnetic field due to the coils is simulated using the FEMM software, which can solve linear and non-linear magnetostatic problems on two-dimensional planar and axisymmetric domains (Meeker, 2018). The z axis in Figure 4 is defined as the symmetry axis. All other boundaries are defined as conducting surfaces.

The plasma particles and fields are simulated using the XOOPIC code (Verboncoeur *et al.*, 1995), which implements the PIC method. In this approach, the positions, and velocities of charged particles are computed from the equations of motion due to the presence of the electric and magnetic fields. The charge density is then discretized to a spatial grid by a weighting process, which allows solving the Poisson equation to obtain new values of the electric potential and the electric field. These fields are then inserted into the equations of motion of the particles, and the cycle is restarted.

3. NUMERICAL RESULTS

Figure 5 shows the axial component of the magnetic field as a function of the axial position z, for r = 0 (i.e., along the centre of the glass tube), measured on the experimental device using a Hall-effect probe, superposed by the magnetic field computed from the numerical model implemented in FEMM. The experiment was conducted using the coil configuration of 10 A. A good agreement between the measured and simulated quantities is evident from this figure. Two local maxima

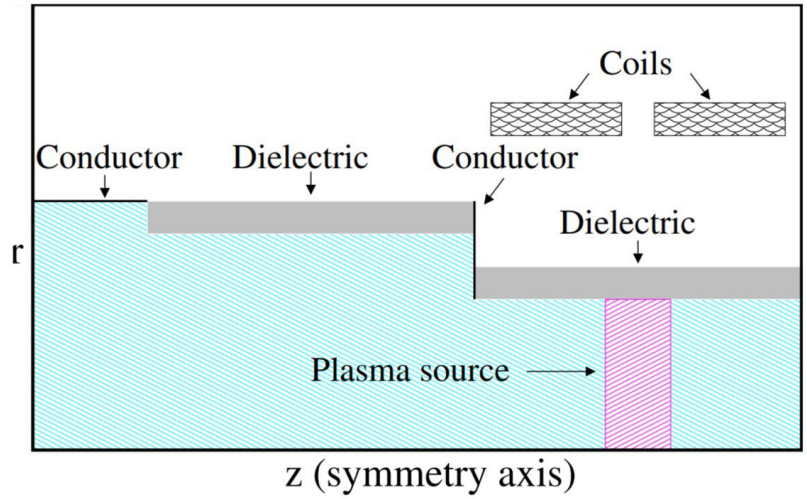

Figure 4. Schematic of the simulation domain, dielectric walls, boundary conditions and the plasma source.

can be distinguished at z ≈ 700 mm and z ≈ 900 mm. These correspond to the field induced by the coils.

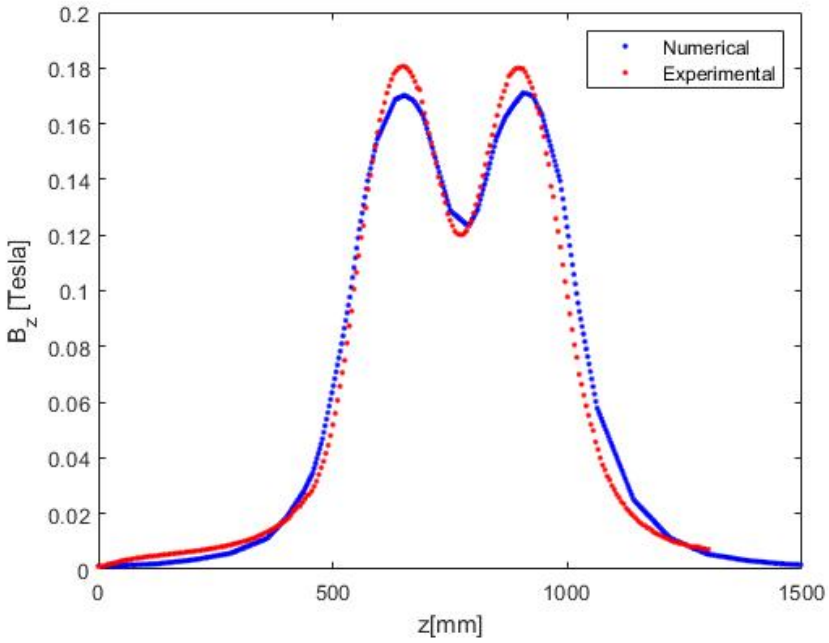

Figure 5. The axial component of the magnetic field as a function of axial position, measured at the center of the glass tube in the experimental device (red circles), and the corresponding values obtained from the numerical simulation (blue circles).

After the removal of the metallic flanges, there could be observed a considerable change in the ions and electrons paths throughout the magnetic lines. Figure 6 represent the new positions of particles and the change of the material show less interference and interaction with the wall as the particles are exhausted from the system, therefore there's a considerable change in the velocity of the particles shown in the following analysis.

Figure 7 shows the axial velocity of ions Vz as a function of z. Plasma particles are inserted around z ≈ 1.1 m, which appears as a region with nearly equal distribution of particles with Vz < 0 and Vz > 0 in all the panels. For z < 1.1 m, most of the particles have Vz < 0, which indicates acceleration towards the exit region. There is a small population of ions near z ≈ 0.7 m with Vz > 0. These are particles that are attracted towards the metal flange between the two quartz tubes. This metal flange has been replaced by a dielectric flange in the experimental device and in the numerical model. A population of accelerated ions with Vz = -10000 m/s can be clearly distinguished for z < 0.6 m. This figure also displays a backflow of ions for z > 1.1, where Vz > 0.

We compute the average value of Vz of ions near the exit region (i.e., with z < 0.3 m). Table 1 displays the average of

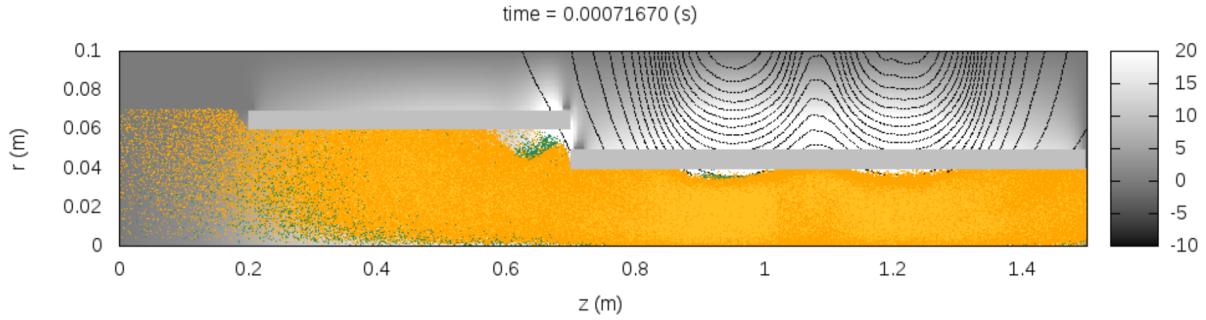

Figure 6. The distribution of plasma particles in the (z, r) simulation domain. Orange dots represent argon ions inserted directly into the simulation, green dots represent electrons, and yellow dots represent ions due to collisions between electrons and the background gas. The gray rectangles represent the walls of the glass tubes, and continuous lines are magnetic field lines due to magnetic coils.

Table 1. Average axial velocity, V_z, for the two configurations.

Coil current (A)	**Ion axial velocity (m/s)**
0 - 5	-8.03×10^3
0 - 20	-7.70×10^3

Vz of two configurations, namely, 10 A and 20 A for the two coils.

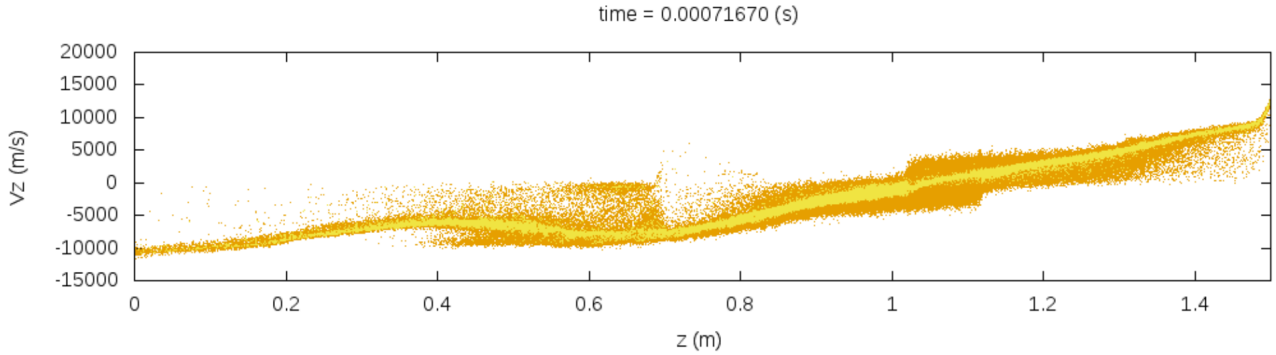

Figure 7. The axial component v_z of the ion velocity as a function of z. Yellow dots represent ions inserted at the source region, and orange dots represent ions inserted via Monte-Carlo collisions between electrons and the background gas.

4. CONCLUSION

In this paper we presented results from an updated version of the HPT-UnB. Enhancements to the experimental device were described, and the numerical model including the simulation domain, boundary conditions for field and particles were described. A good agreement between measured and simulations of the axial component of the magnetic field were obtained. Future work includes measuring temperature values and verifying the presence of different electronic temperature values downstream between the two pairs of coils, and evaluation of propulsion parameters such as thrust and specific impulse.

5. ACKNOWLEDGEMENTS

RAS acknowledges the Master scholarship provided by FAPDF - DPG/UnB Notice No. 0005/2022 - Masters and Doctorate Scholarships 2022/2023 Permanent Postgraduate Development Program of the FAPDF Stricto Sensu – Masters and Doctorate – PDPG. RAM acknowledges support from CNPq, Brazil (grants 407341/2022-6, 407493/2022-0) and COPEI/UnB (grant 7178). JLF acknowledges support from CNPq (grant 405907/2022-2). All numerical simulations were performed using computational resources at the Laboratory for Simulation of Plasma and Electric Propulsion (LaSPPE) at the Institute of Physics, UnB.

6. REFERENCES

Charles, C., 2007. "A review of recent laboratory double layer experiments". *Plasma sources science and technology*, Vol. 16, No. 4, p. R1.

Godyak, V., 2020. "On helicon thrusters: Will they ever fly?" *Journal of Applied Physics*, Vol. 127, No. 10, p. 103301.

Meeker, D.C., 2018. "Finite element method magnetics, version 4.2 (28 feb. 2018 build)". `https://www.femm.info`. Accessed: 2022-06-13.

Miranda, R.A., da Trindade, D.B., Luz, J.M.d.J., da Costa, S. and Ferreira, J.L., 2019. "Particle-in-cell model of the helicon plasma thruster experiment at the university of brasilia". In *Journal of Physics: Conference Series*. IOP Publishing, Vol. 1365, p. 012009.

Pottinger, S., Lappas, V., Charles, C. and Boswell, R., 2011. "Performance characterization of a helicon double layer thruster using direct thrust measurements". *Journal of Physics D: Applied Physics*, Vol. 44, No. 23, p. 235201.

Takahashi, K., Lafleur, T., Charles, C., Alexander, P., Boswell, R., Perren, M., Laine, R., Pottinger, S., Lappas, V., Harle, T. *et al.*, 2011. "Direct thrust measurement of a permanent magnet helicon double layer thruster". *Applied Physics Letters*, Vol. 98, No. 14, p. 141503.

Verboncoeur, J.P., Langdon, A.B. and Gladd, N., 1995. "An object-oriented electromagnetic pic code". *Computer Physics Communications*, Vol. 87, No. 1-2, pp. 199–211.

Williams, L.T. and Walker, M.L., 2013. "Ion production cost of a gridded helicon ion thruster". *Plasma Sources Science and Technology*, Vol. 22, No. 5, p. 055019.

7. RESPONSIBILITY NOTICE

The authors are solely responsible for the printed material included in this paper.